

Study on Asymmetric Deformation Law and Surrounding Rock Control Technology of High Stress Soft Rock Crossing Roadway

Linhao Zhang

School of Energy Science and Engineering, Henan Polytechnic University, Jiaozuo, China
Email: 3144664651@qq.com

How to cite this paper: Zhang, L.H. (2023) Study on Asymmetric Deformation Law and Surrounding Rock Control Technology of High Stress Soft Rock Crossing Roadway. *World Journal of Engineering and Technology*, 11, 353-369.
<https://doi.org/10.4236/wjet.2023.112025>

Received: April 8, 2023

Accepted: May 20, 2023

Published: May 23, 2023

Copyright © 2023 by author(s) and Scientific Research Publishing Inc.
This work is licensed under the Creative Commons Attribution International License (CC BY 4.0).
<http://creativecommons.org/licenses/by/4.0/>



Open Access

Abstract

In order to solve the problem of asymmetric large deformation of high-stress soft rock crossing roadway under complex geological conditions in deep mines, taking the 2# total return airway of 76.2# section of Wuyang Coal Mine as the engineering background, the causes of asymmetric deformation and failure of soft rock crossing roadway in deep mines were summarized and analyzed by means of field investigation, theoretical analysis and numerical simulation, and the asymmetric high-efficiency support technology with large row spacing was studied. The results show that the lithology of roadway strata is the main cause of asymmetric deformation and failure of roadway. The shape change of roadway is not the main influencing factor of asymmetric deformation of roadway, but for the control of roadway surrounding rock, the straight wall semi-circular arch roadway is better than the rectangular roadway. The field industrial test shows that after adopting the new support design scheme, the displacement of the roof and floor of the roadway is reduced by 86.39% compared with the original support design scheme, and the displacement of the two sides of the roadway is reduced by 86.05% compared with the original support design scheme, which can ensure the normal and safe production of the roadway during the service period, and provide reference for the support design of other similar geological conditions.

Keywords

Deep, High Stress, Soft Rock Penetration, Asymmetric Deformation, Support, FLAC3D

1. Introduction

Influenced by the occurrence of environment characteristics of “three highs and

two strong” in the deep coal mine and the complex and abnormal mechanical environment, with the continuous increase of coal mining depth, the surrounding rock of roadway presents the characteristics of strong rheological soft rock, which has the characteristics of fast deformation speed and poor self-stability [1] [2] [3] [4]. Especially for some soft rock crossing roadways under complex geological conditions in deep mines, the surrounding rock of roadway presents the characteristics of asymmetric large deformation and failure as a whole. However, the conventional full-section support not only wastes the support cost, but also cannot effectively control the deformation of surrounding rock of roadway. Therefore, in order to solve the problem of asymmetric large deformation and failure of soft rock crossing roadway, the soft rock crossing roadway is studied. Many experts have conducted in-depth research on it. By studying the asymmetric large deformation roadway of the cross-layer roadway in Xingcun Coal Mine, Wang Jiong [5] *et al.* concluded that the main reason for the asymmetric failure is the dislocation deformation of the roadway. The asymmetric coupling support countermeasures of anchor mesh cable + bottom angle bolt are proposed for the key parts of roadway deformation. Huang Kejun [6] *et al.* studied the inclined roadway of Xujiagou Coal Mine through theoretical analysis and numerical simulation, and proposed that increasing the support density at the roadway layer can effectively control the deformation of roadway surrounding rock. Hao Yuxi [7] *et al.* studied the soft rock cross-layer roadway in the fault fracture zone of Qishan Mine by theoretical analysis and other methods, and concluded that the deformation mechanical mechanism of high-stress expansive soft rock roadway was IABIIABIIIIE composite type. The coupling support control technology of grouting + asymmetric anchor net cable + bottom angle anchor was proposed. Meng Qingbin [8] *et al.* characterized the stress diffusion effect of surrounding rock by the stress expansion coefficient of surrounding rock through theoretical analysis and numerical simulation, and revealed the coupling support effect of bolt and anchor cable pre-tightening force. The feasibility of the combined support technology scheme of bolt-mesh-cable-shotcrete + U-shaped steel support + grouting + floor bolt-grouting distribution was verified by similar simulation test. Sun Shouyi [9] *et al.* proposed the non-uniform reinforcement of the weak structure of the support to strengthen the support of the surrounding rock of the multi-coal seam repeated mining roadway. Zhang [10] *et al.* proposed a segmented reinforcement support scheme through theoretical analysis, numerical simulation and other methods to solve the problem of large deformation of surrounding rock of cross-layer roadway with different vertical depths of coal seam floor under the influence of strong mining, which effectively reduced the deformation and failure range of surrounding rock of cross-layer roadway.

Due to the many influencing factors of deep soft rock crossing roadway, how to effectively control the deformation of surrounding rock during the service period of roadway and select reasonable support methods and support parameters has become the key to ensure the safe use of 2# total return airway in 76.2# sec-

tion of Wuyang Coal Mine during the service period. Therefore, this paper takes the 2# total return airway in the 76.2# section of Wuyang Coal Mine of Shanxi Lu'an Environmental Protection Energy Development Co., Ltd. as the engineering background. Based on the analysis of the influencing factors of asymmetric large deformation and failure of high-stress soft rock cross-layer roadway under complex geological conditions in deep mines, the asymmetric large-row spacing efficient support technology is proposed, and the key parts of the asymmetric large-deformation roadway of soft rock cross-layer are locally strengthened. The original support method of the 2# total return airway in the 76.2# section is optimized by means of numerical simulation software such as FLAC3D, which provides a reference for the surrounding rock support technology of deep soft rock cross-layer asymmetric large-deformation roadway.

2. Engineering Geology Overview

The total design length of 2# total return airway in 76.2# section of Wuyang Coal Mine is 1149 m, which is divided into three sections. The eastern part (outer section) is 75 mining area preparation roadway, the western part is 7503 tile row roadway, the southern part is 7505 transportation roadway, and the northern part is 75 total return airway connection roadway. The eastern part of the middle section is 7505 transportation roadway, the western part is 7505 drainage roadway, the southern part is 7505 goaf, and the northern part is 7503 goaf. The east of Qiqili section is 7505 goaf, the west is 7515 goaf, the south is 76-2# section total return airway, and the north is 7503 goaf, as shown in **Figure 1**.

The design section shape of the roadway (outer section) is straight wall semi-circular arch, the width \times height of the roadway is 5.3 m \times 4.15 m, and the design section shape of the roadway in the middle section is rectangular, the width \times height of the roadway is 5.2 m \times 3.6 m, and the average buried depth is 323.5 m. Driving along the 3# coal seam, the average dip angle of the coal seam along the roadway is -4° . The main roof of the roadway area is sandy mudstone and fine-grained quartz sandstone, the direct roof is mudstone and sandy mudstone, the pseudo roof is carbonaceous mudstone, the direct bottom is sandy mudstone and mudstone, and the old bottom is fine-grained feldspar sandstone. The comprehensive geological histogram is shown in **Figure 2**.

According to three-dimensional seismic exploration: 1) When the roadway is excavated to 34 m ahead of the opening, it will encounter 75-4# normal fault with a rise in front, a drop of 3 m and a dip angle of 65; 2) The roadway excavation to the opening forward 99 m will encounter the 75-4# normal fault with a drop of 3 m and an inclination of 65; 3) When the roadway is excavated to the opening forward about 885 m, it will encounter the Five-201 borehole reverse fault with a drop of 5.5 m and a dip angle of 30; 4) The roadway excavation to the opening forward about 1013 m may encounter the 75-10# normal fault with a drop of about 8 m and a dip angle of 70; 5) When the roadway is excavated to 1034 m ahead of the opening, it may encounter a 76-10# normal fault with a drop of about 8 m and a dip angle of 70° .

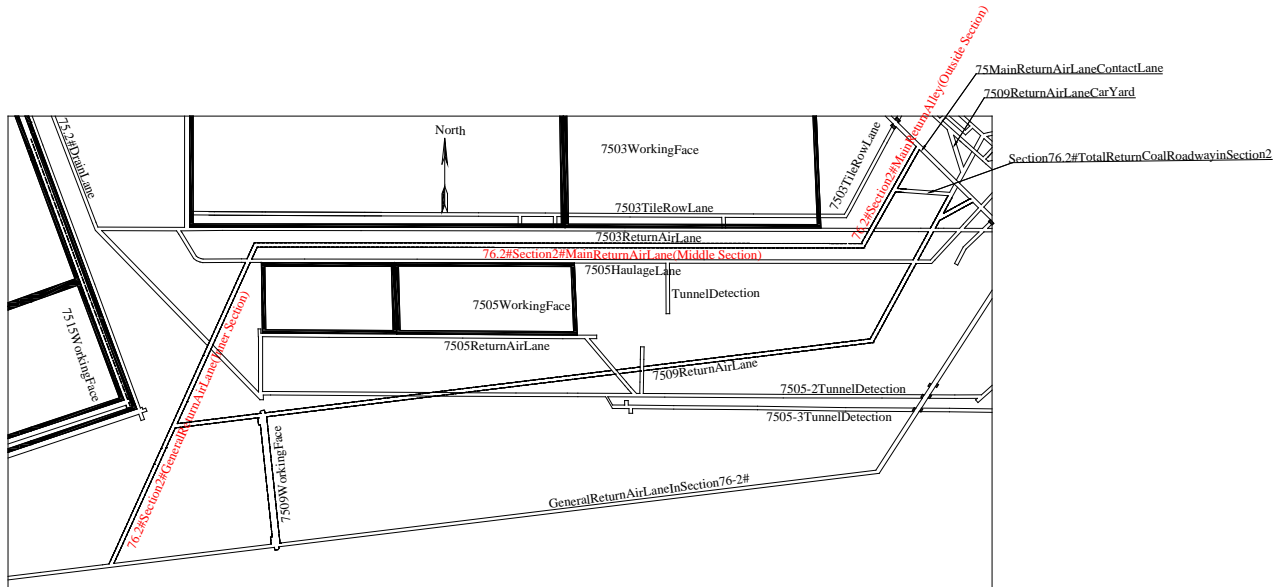


Figure 1. Roadway plane position layout diagram.

Name of roof and floor	Name of coal seam	Columnar	Thickness (m)	Petrographic characteristic
The Old Roof	Sandy mudstone and Fine grain quartz sandstone		$\frac{5.43 \sim 10.25}{7.51}$	Gray white, massive, quartz-based, Calcareous cementation, hard, horizontal bedding, $f=4 \sim 8$.
Immediate Roof	Mudstone and Sandy mudstone		$\frac{2.04 \sim 4.15}{2.96}$	Black, homogeneous, dense, massive, Containing plant fossils, $f=2 \sim 4$.
False Roof	Carbon mudstone		$\frac{0.20 \sim 0.30}{0.25}$	Black, coal line or coal chips, Joint development, easy to fall, $f=2 \sim 3$.
Coal	3# Coal Seam		6.41	Black, medium-thick layered, banded structure, Diamond luster, bright coal, dark coal, semi bright coal The coal quality is PSM.
Direct Bottom	Mudstone and Sandy mudstone		$\frac{2.75 \sim 5.04}{3.84}$	Black, blocky, homogeneous, Containing plant fossil debris, $f=2 \sim 4$.
Old Bottom	The fine feldspathic sandstone		$\frac{4.12 \sim 9.54}{6.52}$	Gray white, feldspar, quartz second, Thick block, black layer, oblique bedding. Calcium cementation, hard, $f=4 \sim 8$.

Figure 2. 76.2# section 2# total return airway comprehensive histogram.

3. Study on Asymmetric Deformation Law of High Stress Soft Rock Crossing Roadway

3.1. Numerical Simulation Scheme Design

The design excavation scheme of 2# total return airway in 76.2# section is as follows: From 76.2# section 2# total return air lane coal roadway stop digging position opening, 1) The same middle line of the return air channel of the 2# main

return air roadway in the 76.2# section goes through the waist line, and the waist line continues to be excavated after encountering the 75-4# fault, with a total of 72.2 meters; 2) In 119.3° in the middle of the waist line driving to the coal seam roof upward 2 m horizon after bedding tunneling, a total of 638.7 meters; 3) According to the -8° waist line driving 60 meters (after driving 43 meters 114.4° inflection) and 7505 transport lane through; 4) Tunneling along the roof of the coal seam, after encountering the reverse fault of the five-201 borehole, the -8° waist line is taken to find the roof of the coal seam to continue the tunneling, a total of 229 meters; 5) After 32 meters of -1° waist line excavation, the unified waist line excavation is connected with the roof of 76.2# total return roadway.

Due to the large difference in the lithology of the surrounding rock of the 2# total return airway in the 76.2# section, the shape of the roadway section is different. Considering the influence of the actual conditions of the specific project and other factors, in order to ensure the reliability of the numerical simulation results, based on the height of the roadway section and the comprehensive geological histogram of the roadway, it can be seen that the rock strata that the roadway passes through are mainly sandy mudstone, fine-grained quartz sandstone and mudstone. Therefore, it is decided to study the influence of the change of the stratum and the shape of the roadway on the distribution law of the stress field of the roadway surrounding rock and the deformation and failure of the roadway surrounding rock. Taking the straight wall semi-circular arch roadway as an example, the specific simulation scheme of the crossing layer is shown in **Table 1**. The simulation diagram of the layer-through scheme is shown in **Figure 3**.

3.2. Establishment of Numerical Simulation Model

The width \times height = 5.3 m \times 4.15 m of the straight wall semi-circular arch roadway in the 2# total return airway of the 76.2# section of the 76.2# section of the Wuyang Coal Mine. The length \times width \times height = 50 m \times 5 m \times 36 m, a total of 27,300 nodes, 22,200 units, limit the bottom and lateral displacement of the model. The overlying rock load q applied on the upper part of the model is about 8.0875 MPa, and the lateral pressure coefficient is $\lambda = 1.0$. The model diagram is shown in **Figure 4**, and the model rock mechanics parameters are shown in **Table 2**.

Table 1. Cross-layer simulation scheme.

Scheme Number	Rock Lithology	Cross-section Shape of Roadway
Scheme 1	Mudstone and sandy mudstone	Straight wall semi-circular arch
Scheme 2	Sandy mudstone and fine-grained quartz sandstone	Straight wall semi-circular arch

Table 2. Mechanical parameters of rock mass model.

Lithologic characters	Parameter	Bulk modulus/GPa	Shear modulus/GPa	Tensile strength/MPa	Cohesion/MPa	Angle of internal friction/	Density/kg/m ³
Fine grain quartz sandstone		6.1	4	1.49	1.5	13	25.7
Sandy mudstone		3.44	2.4	1.1	1.8	17	26
Mudstone		2.5	1.4	0.6	1.67	19	25
Carbon mudstone		2.5	1.4	1.42	2.6	23	26
3# coal seam		2.31	1.6	0.2	1.06	9	14
The fine feldspathic sandstone		10.9	4.9	1.8	1.93	22	27

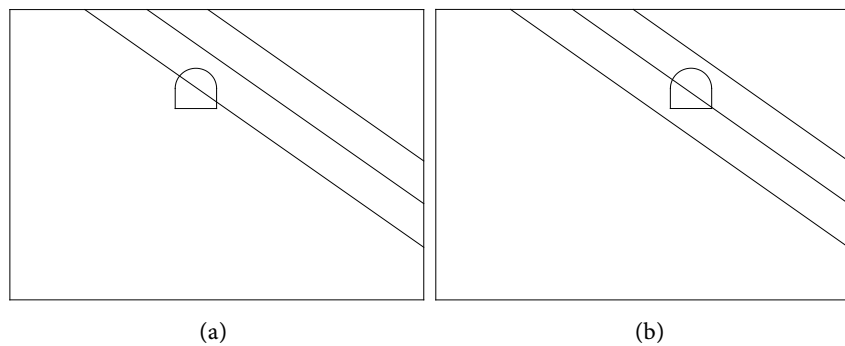


Figure 3. Simulation diagram of layer-through scheme. (a) Cross-layer roadway dominated by mudstone and sandy mudstone; (b) Cross-layer roadway dominated by sandy mudstone and fine-grained quartz sandstone.

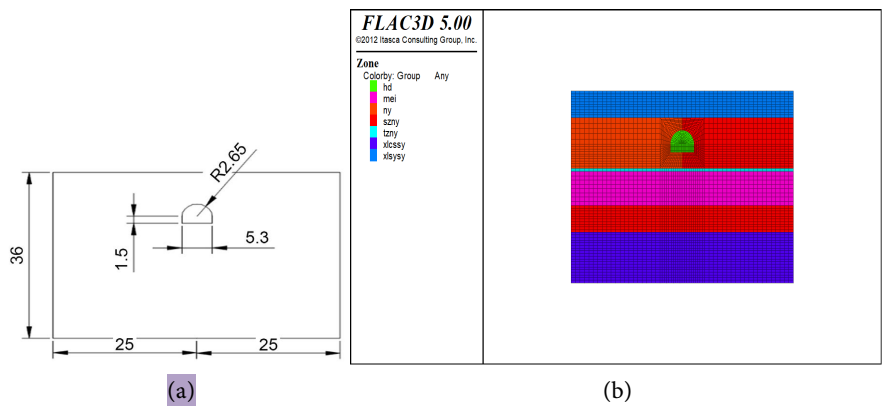


Figure 4. Numerical simulation model of straight wall semicircle arch tunnel. (a) Model simplification diagram; (b) Numerical simulation model diagram.

3.3. Numerical Simulation Results Analysis

3.3.1. Influence of Roadway Layer Change on Stress Field and Deformation Failure of Roadway Surrounding Rock

1) Comparative analysis of roadway displacement characteristics

From **Figure 5** to **Figure 6**, the displacement of the left and right sides of the roof in the cross-layer roadway dominated by mudstone and sandy mudstone is 720 mm and 635 mm, respectively, and the asymmetric deformation is 85 mm.

The displacement of the left and right sides is 416 mm and 265 mm, respectively, and the asymmetric deformation is 151 mm. The roof of the roadway moves to the right as a whole, in the cross-layer roadway dominated by sandy mudstone and fine-grained quartz sandstone, the displacement of the left and right sides of the roof is 744 mm and 770 mm respectively, the asymmetric deformation is 26 mm, the displacement of the left and right sides is 452 mm and 487 mm respectively, and the asymmetric deformation is 35 mm.

In summary, when the lithology of the rock strata where the roadway is located is relatively similar, the overall asymmetry of the roadway is not very obvious, but the deformation of the roadway in soft rock is large, while the deformation in hard rock is small. When the roadway is arranged in soft or hard rock strata, the lithology of the rock strata where the roadway is located has a great influence on the deformation and asymmetric deformation of the roadway, while the lithology of the overlying strata and the underlying strata of the roadway does not play a leading role and has little effect on the roadway.

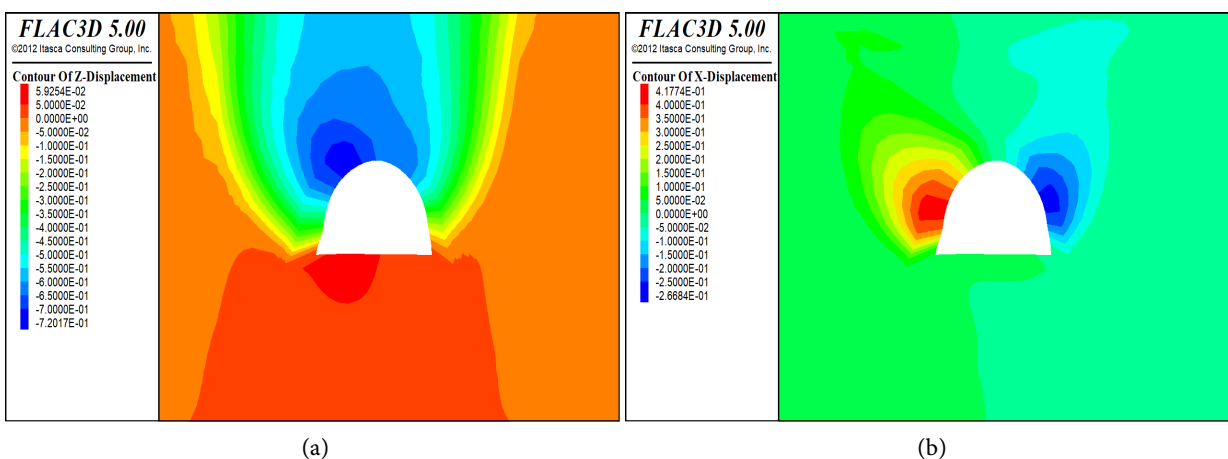


Figure 5. Displacement characteristic nephogram of cross-layer roadway dominated by mudstone and sandy mudstone. (a) Vertical displacement nephogram; (b) Horizontal displacement nephogram.

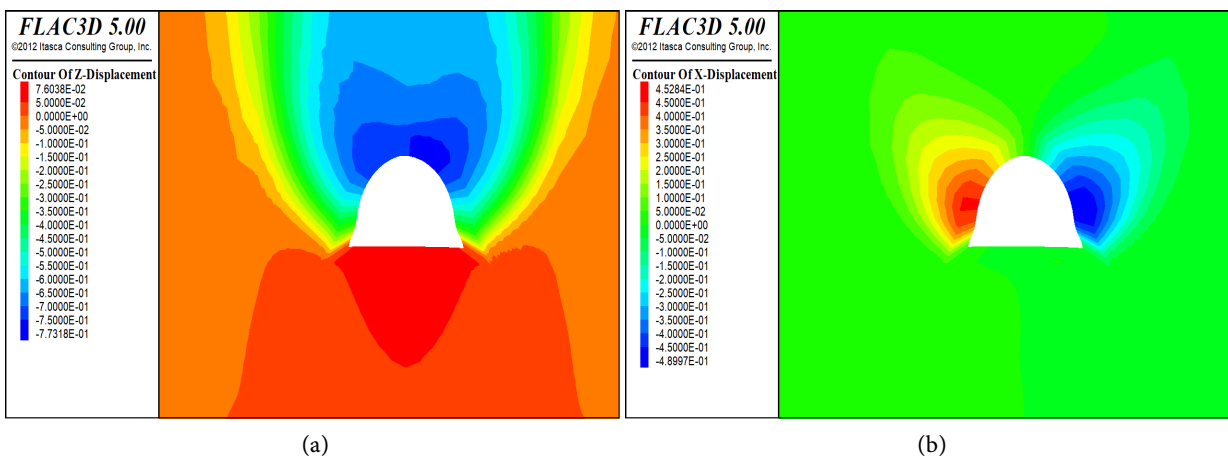


Figure 6. The displacement characteristic cloud diagram of cross-layer roadway mainly composed of sandy mudstone and fine-grained quartz sandstone. (a) Vertical displacement nephogram; (b) Horizontal displacement nephogram.

2) Comparative analysis of roadway stress characteristics

From the analysis of **Figure 7** to **Figure 8**, it can be seen that after the excavation of the roadway, there are different degrees of stress reduction areas around the roadway. Among them, tensile stress areas appear in the roof and floor, and stress concentration areas appear on both sides of the roadway.

In the cross-layer roadway dominated by mudstone and sandy mudstone, the stress on the right side of the roadway is larger than that on the left side, indicating that the stress concentration of the mudstone layer is less than that of the sandy mudstone layer, and the stress concentration range of the mudstone layer is less than that of the sandy mudstone layer. The lithology of the mudstone layer is weak, and it is destroyed under the action of high abutment pressure, losing the bearing capacity, making the stress peak shift to the deep, and at the same time, it breaks and relieves the pressure, releasing the stress of the surrounding rock, reducing the stress concentration in the surrounding rock. In the cross-layer roadway dominated by sandy mudstone and fine-grained quartz sandstone, the roadway can withstand higher abutment pressure due to the strong lithology of fine-grained quartz sandstone and sandy mudstone.

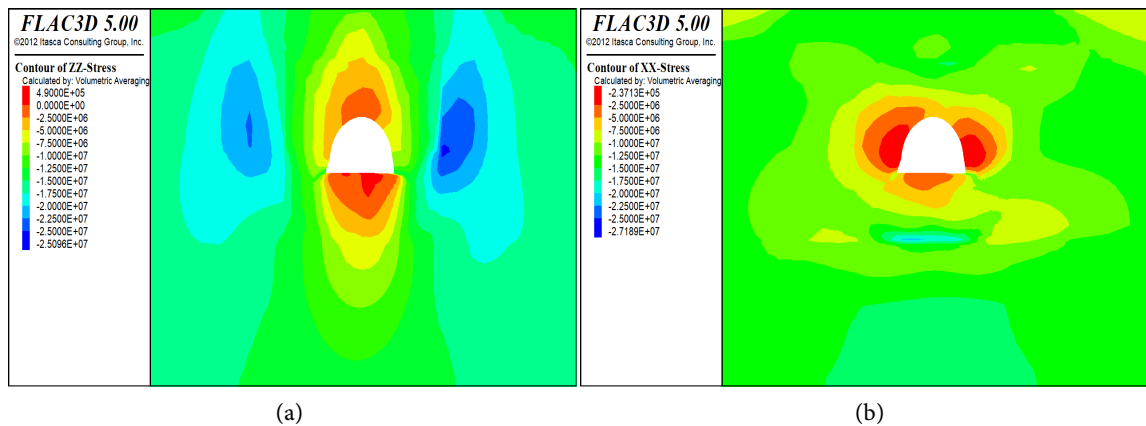


Figure 7. The stress characteristic cloud diagram of cross-layer roadway dominated by mudstone and sandy mudstone. (a) Vertical stress nephogram; (b) Horizontal stress nephogram.

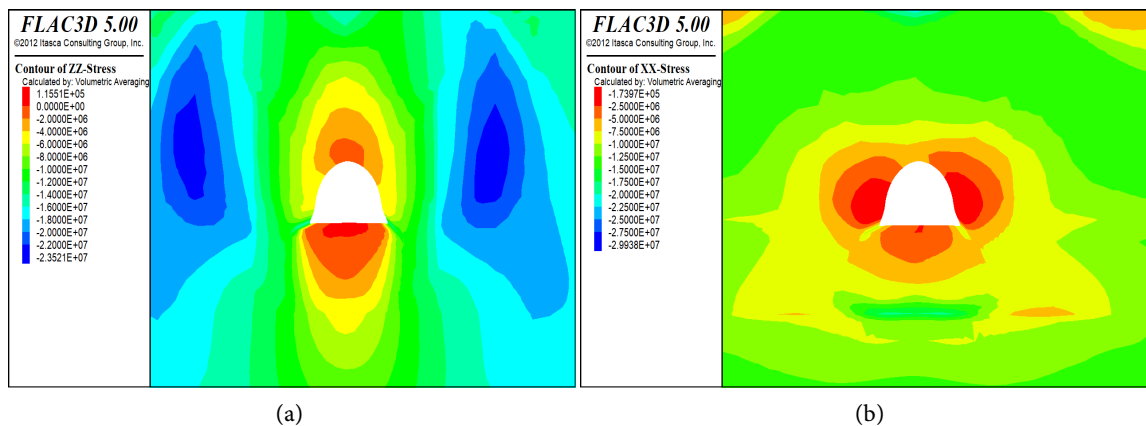


Figure 8. The stress characteristic cloud diagram of cross-layer roadway dominated by sandy mudstone and fine-grained quartz sandstone. (a) Vertical stress nephogram; (b) Horizontal stress nephogram.

Therefore, the internal stress distribution range of the roadway is significantly larger than that of the cross-layer roadway dominated by mudstone and sandy mudstone.

In summary, the lithology of the rock stratum where the roadway is located plays a leading role in the asymmetric distribution of the roadway, and the soft rock roadway is damaged due to the difficulty of bearing high stress, which makes the stress transfer to the interior. When the rock stratum of the roadway is hard rock, the roadway bears high stress concentration and the integrity of the surrounding rock is good.

3.3.2. The Influence of Roadway Shape Change on the Stress Field and Deformation of Roadway Surrounding Rock

Using the control variable method, when the rock lithology parameters of the surrounding rock of the roadway are consistent, and the cross-section shape of the roadway is changed to rectangular width \times height = 5.3 m \times 4.15 m, the displacement cloud map is shown in **Figure 9**, **Figure 10**.

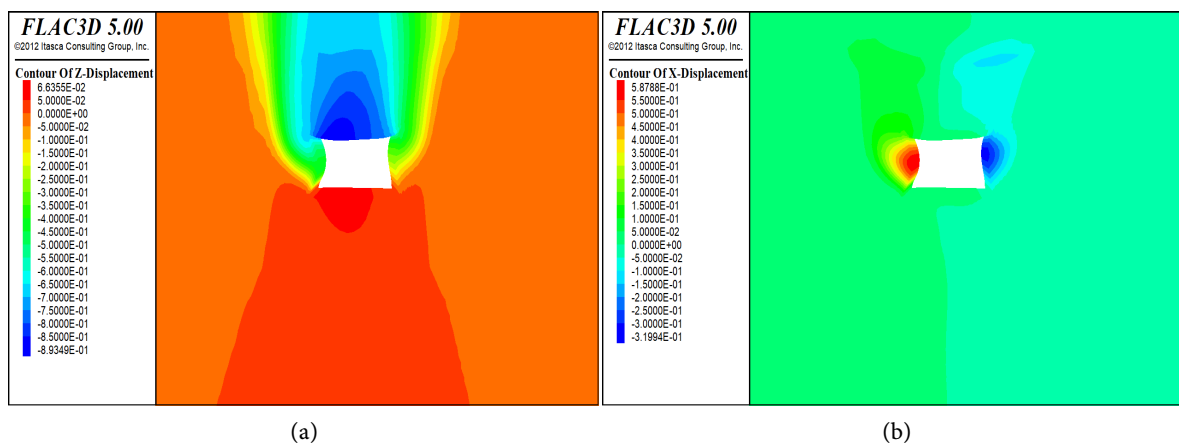


Figure 9. Displacement nephogram of cross-layer roadway dominated by mudstone and sandy mudstone. (a) Vertical displacement nephogram; (b) Horizontal displacement nephogram.

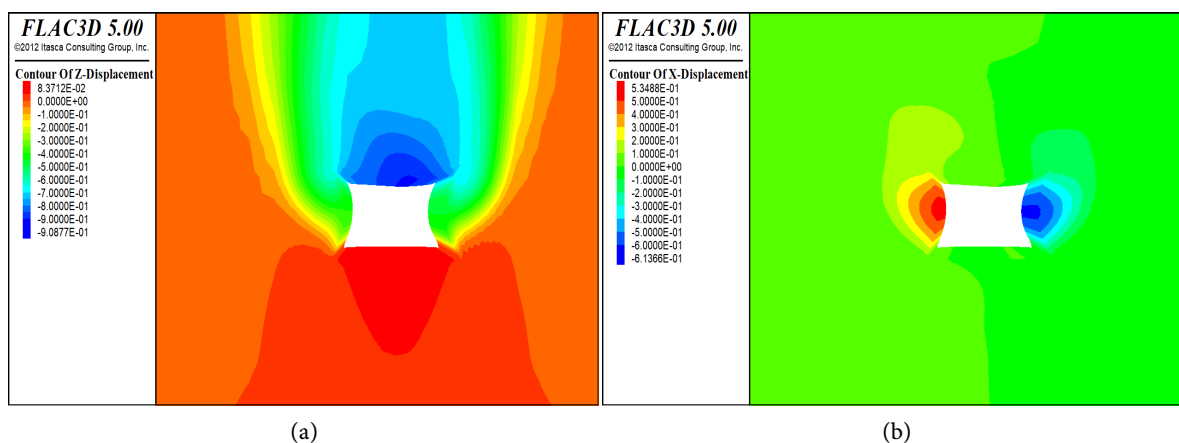


Figure 10. Displacement characteristic nephogram of cross-layer roadway dominated by sandy mudstone and fine-grained quartz sandstone. (a) Vertical displacement nephogram; (b) Horizontal displacement nephogram.

According to the analysis of **Figure 9**, **Figure 10**, the displacement of the left and right sides of the roof in the cross-layer roadway dominated by mudstone and sandy mudstone is 893 mm and 782 mm respectively, and the asymmetric deformation is 111 mm. The displacement of the left and right sides is 586 mm and 311 mm respectively, and the asymmetric deformation is 275 mm, and the roof of the roadway is shifted to the right as a whole. In the cross-layer roadway mainly composed of sandy mudstone and fine-grained quartz sandstone, the displacement of the left and right sides of the roof is 840 mm and 880 mm respectively, and the asymmetric deformation is 40 mm. The displacement of the left and right sides is 534 mm and 613 mm respectively, and the asymmetric deformation is 79 mm. The roof moves to the left as a whole, and the roof displacement near the sandy mudstone side is the largest.

Taking the cross-layer roadway dominated by mudstone and sandy mudstone as an example, by comparing the asymmetric deformation of roadways with different cross-section shapes, as shown in **Figure 11**. It can be obtained that when the shape of the roadway changes, the asymmetric deformation of the roof and floor of the roadway does not change significantly, but the asymmetric deformation of the side of the straight wall semi-circular arch roadway is significantly lower than that of the rectangular roadway, and the deformation of the surrounding rock of the straight wall semi-circular arch roadway is smaller than that of the rectangular roadway, indicating that the shape change of the roadway is not the main influencing factor of the asymmetric deformation of the roadway, but the shape change of the roadway has a certain influence on controlling the deformation of the roadway.

4. Research on Surrounding Rock Control Technology of Cross-Layer Roadway

4.1. Numerical Simulation Scheme Design

For the semi-circular arch roadway with straight wall, the preliminary design adopts the combined support system of resin lengthening and anchoring strong bolt and anchor cable. Taking mudstone and sandy mudstone as the main crossing roadway as an example, two kinds of support design schemes are proposed. The numerical simulation model is shown in **Figure 4**, and the mechanical parameters of rock mass in the model are shown in **Table 2**. The specific parameters are as follows:

1) Support design scheme 1: The $\Phi 18.9 \times 6300$ mm anchor cable is arranged in the vault by “2-3-2” mode, and the resin is used to lengthen the anchorage. The anchorage length is 1921 mm, the anchor cable spacing is 2.0 m, and the row spacing is 1.0 m. There is one anchor cable on each side of the first row, one anchor cable on the middle of the arch, and one anchor cable on each side of the center. Two $\Phi 22 \times 2400$ mm bolts are arranged on each side of the straight wall, and the resin is used to lengthen the anchorage. The anchorage length is 1208 mm, the anchorage force is 200 kN, the bolt spacing is 0.9 m, and the row spacing is 1.0 m, as shown in **Figure 12(a)**.

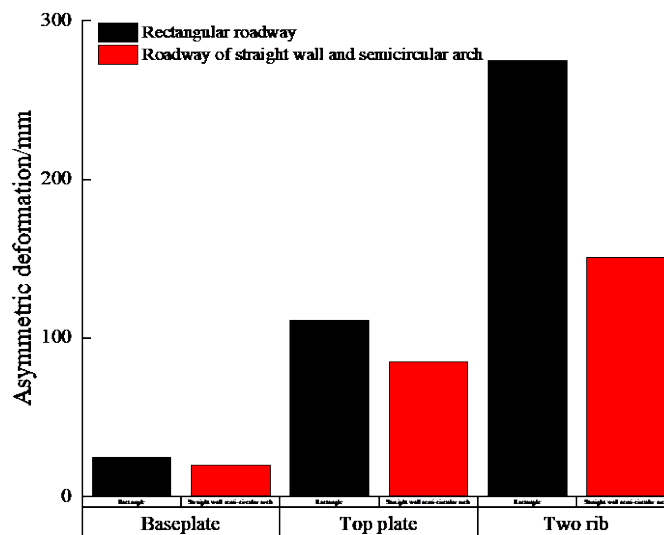


Figure 11. Asymmetric deformation of different section shapes in roadway.

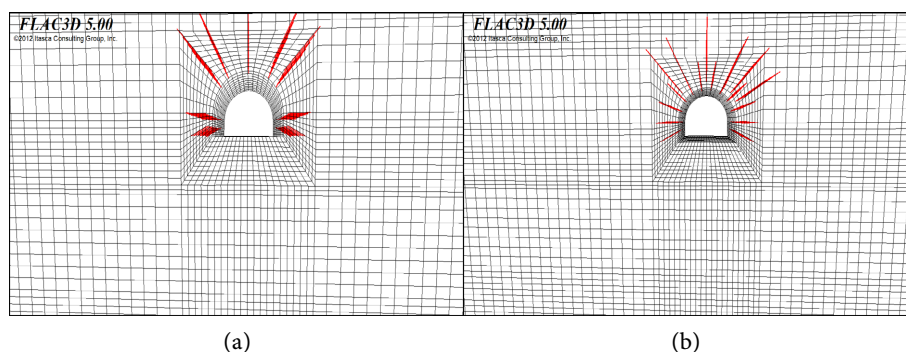


Figure 12. Numerical simulation diagram of arch roadway support. (a) Support design scheme 1; (b) Support design scheme 2.

2) Support design scheme two: Straight wall support design parameters and support design scheme is consistent, the local strengthening support is carried out on the vault, and the arrangement of the vault anchor cable in the first support design scheme is changed to “3-4-3” arrangement, that is, one anchor cable is set in the middle of the first row of arches, one anchor cable is set on each side with a distance of 2.0 m, one anchor cable is set on each side with a distance of 1.0 m, and one anchor cable is set on each side with a distance of 2.0 m. Nine $\Phi 22 \times 2400$ mm bolts are arranged on the vault, with a spacing of 0.9 m and a row spacing of 1.0 m, as shown in **Figure 12(b)**.

4.2. Numerical Simulation Results Analysis

4.2.1. Comparative Analysis of Roadway Surrounding Rock Stress Characteristics

From **Figure 13** to **Figure 14**, it can be seen that due to the different lithology of the rock strata in the crossing section of the roadway, the stress concentration on the left and right sides of the roadway is quite different, and the stress around the roadway is asymmetrically distributed. The peak value of the main stress

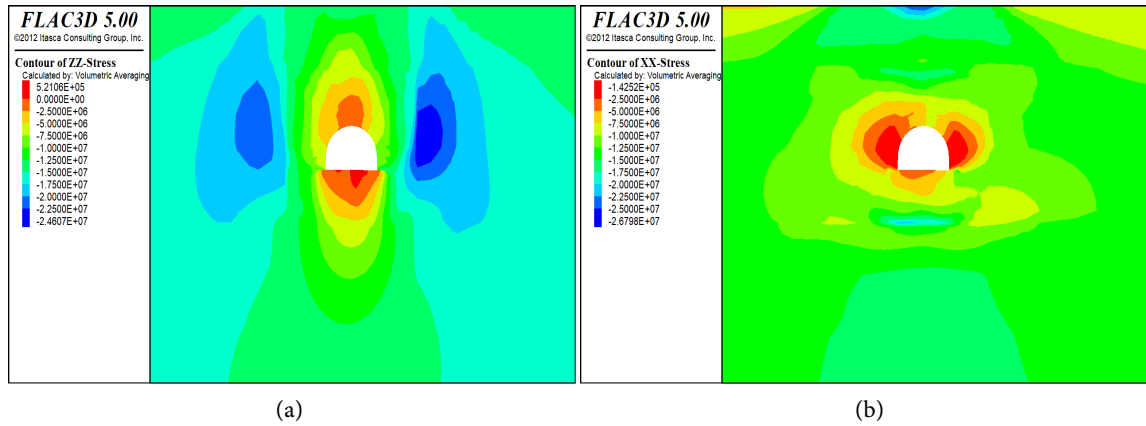


Figure 13. Supporting design scheme-roadway stress characteristic cloud chart. (a) Vertical stress nephogram; (b) Horizontal stress nephogram.

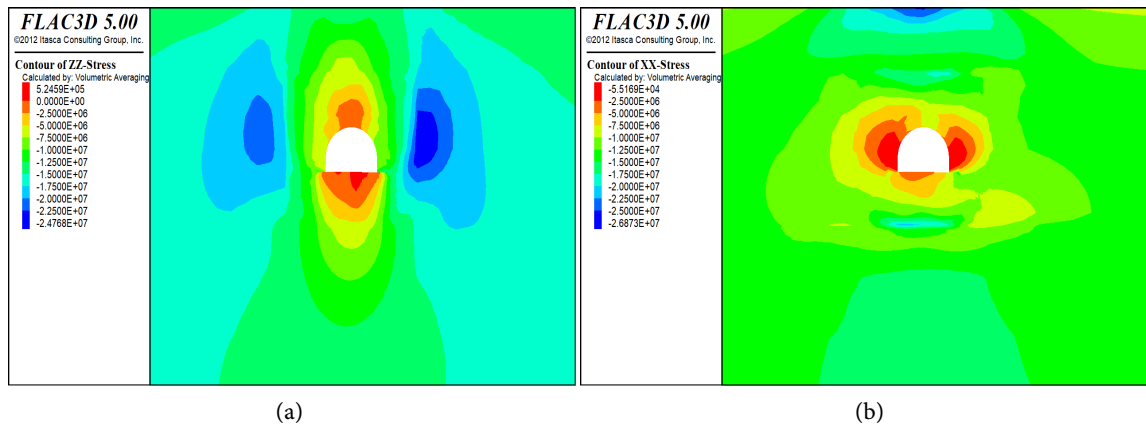


Figure 14. Support design scheme two roadway stress characteristic cloud map. (a) Vertical stress nephogram; (b) Horizontal stress nephogram.

concentration on the left side of the roadway is 22.9695 MPa, and the peak value of the main stress concentration on the right side is 25.0272 Mpa. With the increase of support strength, the peak value of the principal stress on the two sides of the roadway obviously moves to the surface of the roadway, indicating that the stress of the surrounding rock of the roadway is obviously improved.

4.2.2. Comparative Analysis of Displacement Characteristics of Roadway Surrounding Rock

From **Figure 15** to **Figure 16**, it can be obtained that when the support design scheme is adopted, although the roof displacement and the left and right sides displacement are improved to a certain extent, the roof displacement is still 122 mm and the left side displacement is 100 mm, which fails to ensure the safe use of the roadway. When the support design scheme is adopted, the displacement of the roof is reduced to 50 mm, the displacement of the left side is reduced to 60 mm, and the displacement of the right side is reduced to 34 mm, which can significantly improve the displacement of the roof and floor of the roadway and the displacement of the left and right sides. It meets the requirements of the specifi-

cation and can effectively control the deformation of the roof and floor of the roadway and the two sides.

In summary, the roadways in different cross-sections show asymmetric deformation characteristics. The larger the lithology difference of the surrounding rock strata of the roadway, the more obvious the asymmetry phenomenon, and the larger the asymmetric deformation of the roadway. When the support design scheme is adopted, the support design effect is more obvious. The dynamic asymmetric local reinforcement support can give full play to the support performance of the support structure and ensure the safety of the roadway.

5. Actual-Service Test

5.1. Determination of Supporting Design Scheme

Combined with numerical simulation research, the support scheme of straight wall semi-circular arch roadway is determined as shown in **Figure 17**, and the specific support parameters are designed as follows:

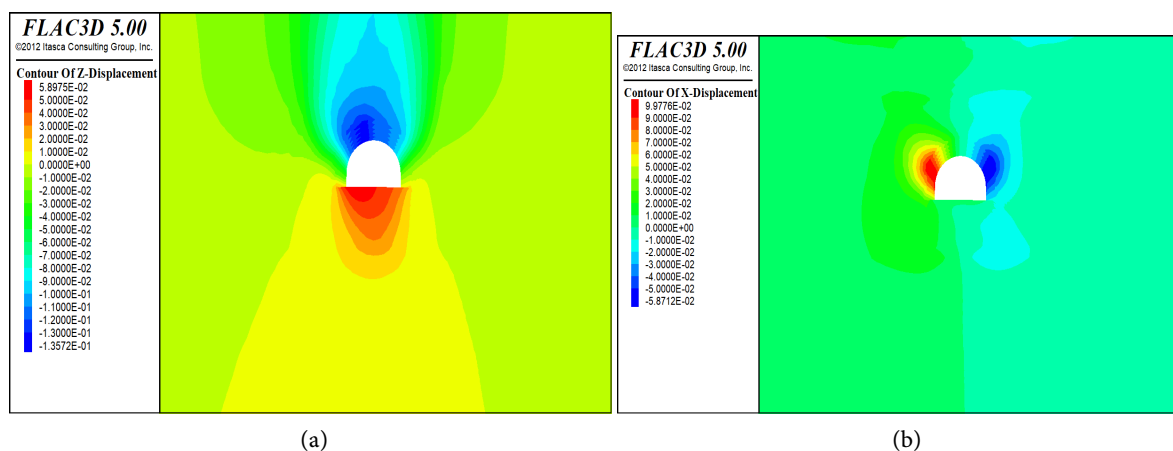


Figure 15. Supporting design scheme-roadway displacement characteristic cloud chart. (a) Vertical displacement nephogram; (b) Horizontal displacement nephogram.

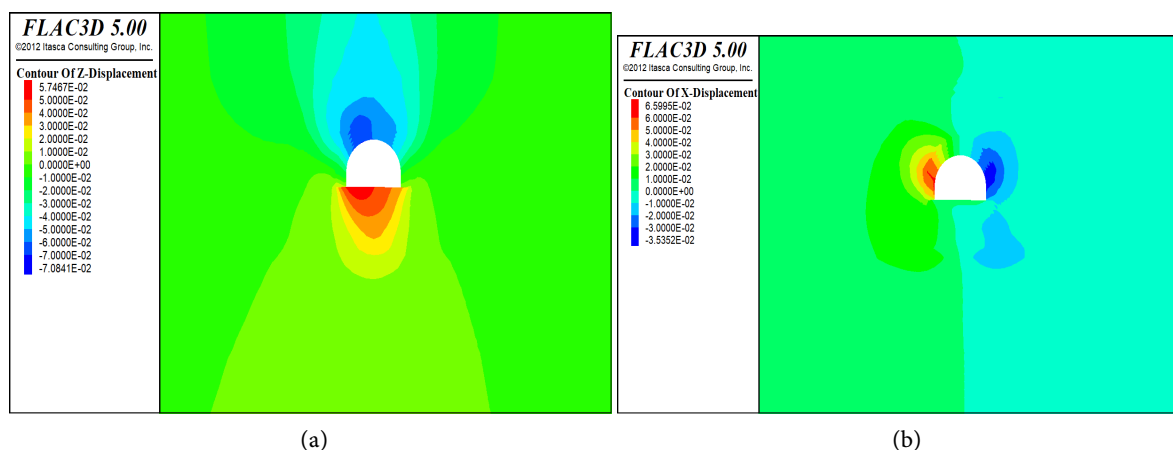


Figure 16. Support design scheme two roadway displacement characteristic cloud map. (a) Vertical displacement nephogram; (b) Horizontal displacement nephogram.

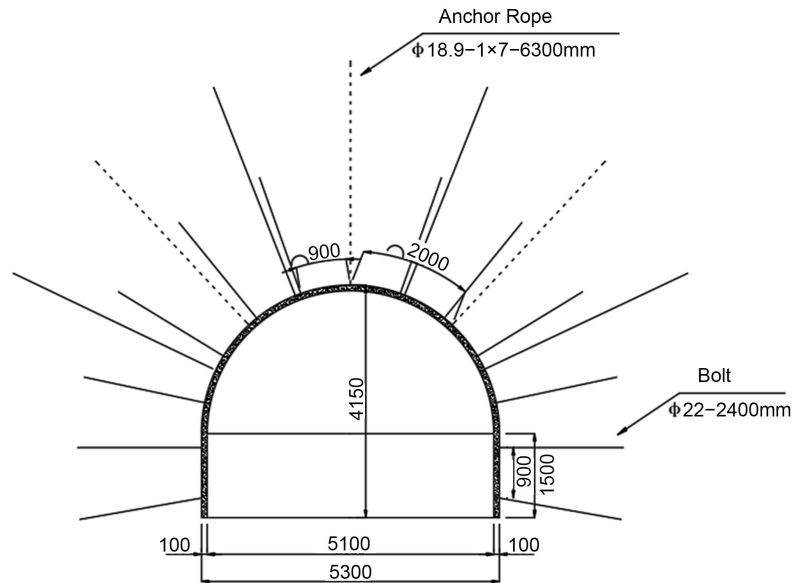


Figure 17. Straight wall semi-circular arch roadway bolt, anchor cable layout diagram.

1) Design of vault support parameters:

Anchor form and specifications: The rod body is 22# left-handed non-longitudinal rib thread steel bar, the steel number is 500, the length is 2.4 m, and the tail thread is M24.

Anchoring method: Long resin anchorage, using two anchorage agent, a specification for MSCKb2335, another specification for MSZK360. The borehole diameter is 30 mm, the anchorage length is 1208 mm, and the anchorage force is 200 kN.

Specification of steel joist: Two $\Phi 16$ mm, 100 mm width, 3.8 m length of double steel joist lap used.

Anchor arrangement: The bolt row spacing is 1.0 m, 9 bolts per row, and the spacing is 0.9 m.

Mesh specification: The material is 10# iron wire, mesh size 40×40 mm, mesh size 4.5×1.1 m, connected with 16# lead wire, double wire double buckle, hole connected.

Cable form and specifications: The cable material is $\Phi 18.9$ mm, 1×7 high-strength low-relaxation prestressed steel strands, with a length of 6.3 m and a diameter of 28 mm. One MSCKb2335 and two MSK2360 resin coils are used for anchoring, and the anchorage length is 1921 mm.

Anchor cable arrangement: The spacing is 2.0 m, the row spacing is 1.0 m, and the 3-4-3 arrangement is arranged (one in the middle of the first row of arches, one in each side with a spacing of 2.0 m, one in each side of the second row with a center deviation of 1.0 m, and one in each side with a spacing of 2.0 m).

2) Straight wall support parameter design:

Anchor form and specifications: The rod body is 22# left-handed non-longi-

tudinal rib thread steel bar, the steel number is 500, the length is 2.4 m, and the tail thread is M24.

Anchoring method: The resin lengthened anchorage adopts two anchorage agents, one is MSK2335 and the other is MSZ2360. The borehole diameter is 30 mm, the anchorage length is 1208 mm, and the anchorage force is 200 kN.

Specification of steel bar joist: It is welded with $\Phi 16$ mm steel bar, with a width of 100 mm and a length of 1.1 m.

Angle of bolt: The lower bolt is set 10° away from the outside, and the upper bolt is set perpendicular to the roadway side.

Mesh specification: The material is 10# iron wire, the mesh size is 40×40 mm, and the mesh size is 1.3×1.1 m connected with 16# lead wire, double wire double buckle, hole connected.

Anchor arrangement: The bolt row spacing is 1.0 m, 2 bolts per row, and the spacing is 0.9 m.

5.2. Industrial Testing

In order to verify the specific support effect of the support design scheme, two stations were arranged at 50 m and 100 m of the 2# total return airway in the 76.2# section by using the “cross” distribution method for 30 days of roadway surface displacement monitoring. The results of the observation data of the two stations at 1# ~ 2# stations are shown in **Figure 18**.

From **Figure 18**, it can be seen that in the first 12 days, the deformation rate of the surrounding rock of the two sides of the roadway and the deformation rate of the surrounding rock of the roof and floor are at the maximum value, and the maximum average deformation rate is 7.23 mm/d and 8.62 mm/d respectively. After 12 days, the deformation of the roadway continues to increase, but the overall deformation rate slows down. After 21 days, the deformation rate of the roof and floor of the roadway and the two sides gradually stabilizes, and the

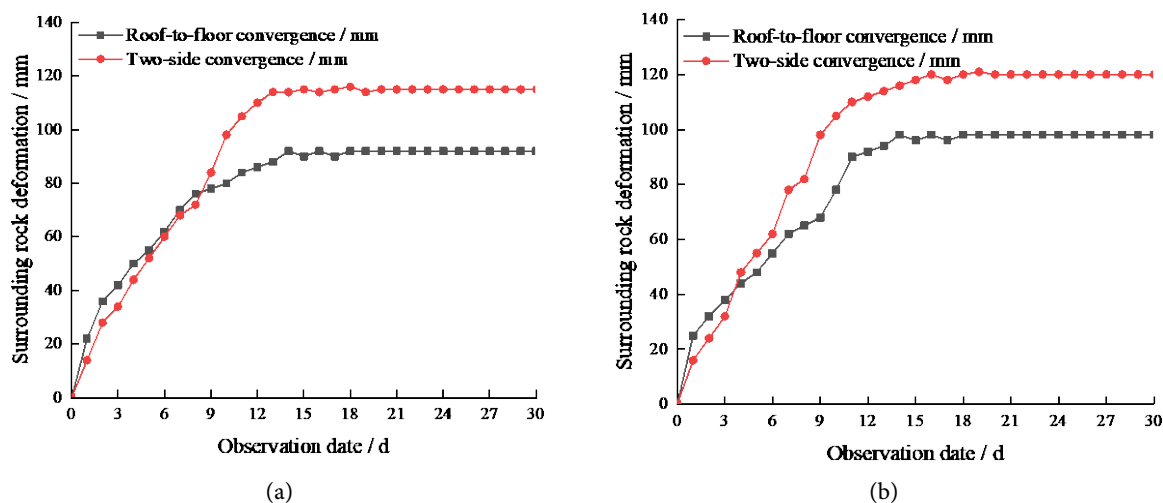


Figure 18. Roadway surrounding rock monitoring curve. (a) 1# station roadway surrounding rock deformation/mm; (b) 2# station roadway surrounding rock deformation/mm.

deformation of the surrounding rock of the roadway basically has no obvious change. The maximum displacement of the roof and floor is 98 mm, which is 86.39% lower than the original 720 mm; the maximum displacement of the two sides is 120 mm, which is 86.05% lower than the original 860 mm. The displacement of the roof and floor of the roadway and the displacement of the two sides are obviously reduced after the second support design scheme is adopted. In particular, the asymmetric deformation of the surrounding rock of the two sides of the roadway is obviously improved, and the stability of the surrounding rock is significantly improved, indicating that the new support design scheme can effectively control the deformation of the surrounding rock of the roadway.

6. Conclusions

1) The influence of roadway horizon change and shape change on asymmetric deformation law is analyzed: a) When the roadway is arranged in a softer or harder rock layer, the lithology of the rock layer where the roadway is located plays a leading role in the asymmetric distribution of the roadway, while the lithology of the overlying rock layer and the underlying rock layer has less influence on the roadway. b) When the lithology of the rock strata where the roadway is located is relatively similar, the overall asymmetry of the roadway is not obvious, and the soft rock roadway is damaged due to the difficulty of bearing high stress, which makes the stress transfer to the interior and the roadway deformation large. When the rock strata of the roadway are hard rock, the roadway bears high stress concentration and the integrity of the surrounding rock is good. c) The shape change of roadway is not the main influencing factor of asymmetric deformation of roadway, but the straight wall semi-circular arch roadway is better than the rectangular roadway in the same lithology.

2) Using FLAC3D numerical simulation for comparative analysis: The roadways in different strata show the characteristics of asymmetric deformation. The greater the difference in the lithology of the surrounding rock of the roadway is, the more obvious the asymmetry is, and the larger the asymmetric deformation of the left and right sides is. When the supporting design scheme is adopted, the supporting design effect is more obvious. The dynamic asymmetric local strengthening support can give full play to the supporting performance of the supporting structure and ensure the safety of the roadway.

3) The industrial test shows that the second support design scheme can effectively control the deformation of roadway surrounding rock, and the maximum displacement of roof and floor is 98 mm, which is 86.39% lower than that of the original support design scheme. The maximum displacement of the two sides is 120 mm, which is 86.05% less than that of the support design scheme. The support design scheme 2 has achieved remarkable results and can effectively control the deformation of the surrounding rock of the roadway.

Acknowledgements

This work was financially supported by the Special Project of Basic Research

Funds for Universities (NSFRF140134).

Conflicts of Interest

The author declares no conflicts of interest regarding the publication of this paper.

References

- [1] Kang, H.P. (2021) 70 Years of Development and Prospect Of Surrounding Rock Control Technology in Coal Mine Roadway in China. *Journal of Rock Mechanics and Engineering*, No. 1, 1-30.
- [2] Hou, C.J., Wang, X.Y., Bai, J.B., Meng, N.K. and Wu, W.D. (2021) Basic Theory and Technology of Surrounding Rock Stability Control in Deep Roadway. *Journal of China University of Mining and Technology*, No. 1, 1-12.
- [3] Huang, Q.X. (2021) Study on Coordinated Control of Internal and External Bearing Capacity of Typical Deep Roadway Surrounding Rock in Pingdingshan Mining Area. Doctoral Dissertation, China University of Mining and Technology, Xuzhou. <https://kns.cnki.net/KCMS/detail/detail.aspx?dbname=CDFDLAST2022&filename=1021773585.nh>
- [4] Yu, C.S., Wei, S.J., Zhang, S., Wang, M. and Shen, W.L. (2021) Failure Characteristics and Strong Anchoring Control Technology of Surrounding Rock in Deep Coal Seam Roadway. *Journal of Henan University of Technology (Natural Science Edition)*, No. 4, 28-37.
- [5] Wang, J., Guo, Z.B., Cai, F., Hao, Y.X. and Liu, X. (2014) Research on Asymmetric Deformation Mechanism and Control Countermeasures of Deep Cross-Layer Roadway. *Journal of Mining and Safety Engineering*, No. 1, 28-33.
- [6] Huang, K.J., Li, L., Liu, W.J., Wang, P. and Wang, W.Q. (2014) Numerical Simulation Analysis of Failure Mechanism and Support Stability of Cross-Layer Inclined Roadway in High Stress Soft Rock Area. *Mining Safety and Environmental Protection*, No. 2, 35-40.
- [7] Hao, Y.X., Wang, J., Wang, H., Meng, Z.G. and Guo, Z.B. (2016) Coupling Control Measures of Anchor, Mesh and Cable in Deep Fault Fracture Zone through Layer Soft Rock Roadway. *Journal of Mining and Safety Engineering*, No. 2, 231-237.
- [8] Meng, Q.B., Han, L.J., *et al.* (2017) Research and Application of Coupling Support Effect of Deep High Stress Soft Rock Roadway. *Geotechnical Mechanics*, No. 5, 1424-1435 + 1444.
- [9] Sun, S.Y., Zhao, C.Z., *et al.* (2020) Study on Deformation Characteristics and Repair and Reinforcement Technology of Surrounding Rock of Cross-Layer Roadway in Multi-Coal Seam Repeated Mining. *Journal of Mining and Safety Engineering*, No. 4, 681-688.
- [10] Zhang, T.L., Ning, S. and Zhang, C. (2021) Subsection Support Technology of Surrounding Rock in Coal Seam Floor Crossing Roadway. *Mining Research and Development*, No. 10, 115-120.